Published in final edited form as:
Neuron. 2014 November 19; 84(4): 857–869. doi:10.1016/j.neuron.2014.10.012.

Configural and elemental coding of natural odor mixture components in the human brain

James D. Howard[1] and **Jay A. Gottfried**[1,2,3]

[1]Department of Neurology, Northwestern University Feinberg School of Medicine, Chicago, IL, USA

[2]Cognitive Neurology & Alzheimer's Disease Center, Northwestern University Feinberg School of Medicine, Chicago, IL, USA

[3]Department of Psychology, Northwestern University Weinberg College of Arts and Sciences, Evanston, IL, USA

SUMMARY

Most real-world odors are complex mixtures of distinct molecular components. Olfactory systems can adopt different strategies to contend with this stimulus complexity. In elemental processing, odor perception is derived from the sum of its parts; in configural processing, the parts are integrated into unique perceptual wholes. Here we used gas-chromatography/mass-spectrometry techniques to deconstruct a complex natural food smell and assess whether olfactory salience is confined to the whole odor or is also embodied in its parts. By implementing an fMRI sensory-specific satiety paradigm, we identified reward-based changes in orbitofrontal cortex (OFC) for the whole odor and for a small subset of components. Moreover, component-specific changes in OFC-amygdala connectivity correlated with perceived value. Our findings imply that the human brain has direct access to the elemental content of a natural food odor, and highlight the dynamic capacity of the olfactory system to engage both object-level and component-level mechanisms to subserve behavior.

INTRODUCTION

An essential function of the brain is to encode and interpret the behavioral salience of stimuli encountered in the environment. Because the natural form of real-world stimuli is often a mixture or composite of physical features, sensory systems are confronted with the goal of synthesizing stimulus parts into perceptual wholes that retain ecological relevance for the perceiver. However, in many instances, behavioral salience can be embodied in the

Corresponding author contact information: james-howard@northwestern.edu, Phone: (617) 594-9533, Address: Northwestern University Feinberg School of Medicine, Department of Neurology, 303 E. Chicago Ave., Ward 10-144, Chicago, IL 60611.

AUTHOR CONTRIBUTIONS

J.D.H. and J.A.G. designed the experiment. J.D.H. collected and analyzed the data. J.D.H. and J.A.G. prepared the manuscript.

parts themselves, placing additional demands on sensory systems to read out and represent information about stimulus components.

The competition between component analysis and feature integration– that is, between parts and wholes – can be framed in terms of *elemental* and *configural* modes of perceptual processing. While many theoretical accounts suggest that one or the other system has exclusive influence over perception (Pearce, 1994; Rescorla and Wagner, 1972), some models propose that task demands determine whether elemental or configural processing is engaged at any given time (Honey et al., 2014; Melchers et al., 2008). An example of such dual-mode processing in humans comes from studies of the visual system, which is capable of encoding the combined features of a complex face image as a configural representation (Kanwisher et al., 1997), but can also extract elemental content of the same image from just the eyes alone (Whalen et al., 2004).

In the case of the olfactory system, naturally occurring odors provide a unique opportunity to investigate the neural dynamics of elemental and configural processing. The majority of realworld smells are composed of complex mixtures of dozens, if not hundreds, of unique molecular components, each of which can in turn be described by myriad physicochemical parameters. Perhaps not surprisingly then, central processing of multidimensional odor stimuli is highly configural, such that complex odor mixtures are perceived as unified wholes, with no conscious access to physical stimulus features (Kay et al., 2005; Laing and Francis, 1989; Snitz et al., 2013).

Piriform cortex (PC), a target of both afferent input from the olfactory bulb (OB) and associative input from higher-order brain areas including orbitofrontal cortex (OFC), is principally involved in olfactory configural coding. Animal studies indicate that mixtures of odorants evoke response patterns in PC that qualitatively differ from those evoked by the individual odorants. Moreover, these mixture-based responses cannot be reconstituted by combining responses to each odorant, implying that piriform representations of complex mixtures reflect more than the mere sum of the parts (Barnes et al., 2008; Stettler and Axel, 2009; Yoshida and Mori, 2007).

Interestingly, a separate line of investigation has shown that individual components found in natural odors can support stereotypical behavioral responses evoked by the mixture wholes. In mice, a select volatile of male urine, (methylthio)methanethiol, was sufficient to enhance odor investigation times in female mice (Lin et al., 2005); in moths, odor components of the sacred *Datura* flower, including benzaldehyde, benzyl alcohol, and linalool, provoked feeding and flight behaviors that were indistinguishable from the whole floral fragrance (Riffell et al., 2009). In both cases neural representations of component coding were identified in early olfactory processing areas of the mouse OB or the insect analog in the antennal lobe. These studies raise the possibility that, despite the apparent predominance of configural processing in the olfactory system, behaviorally relevant information can be extracted from distinct subsets of molecular components within a natural odor mixture. Whether the human brain similarly has access to elemental odor mixture information is not known.

While the smell of mouse urine or *Datura* fragrance carries specific ecological relevance for mice and moths, they are unlikely to have a similar potency for humans. However, one category that holds certain sway over human behavior is food aromas, which can serve as a powerful signal to both initiate and terminate feeding (Saper et al., 2002; Shepherd, 2006). Moreover, the rewarding properties of a particular food odor can be selectively manipulated if the corresponding food is eaten to satiety, a phenomenon known as olfactory sensory-specific satiety (Rolls and Rolls, 1997), providing a robust experimental assay with direct relevance for an essential human behavior.

Here we used gas chromatography/mass spectrometry (GC/MS) to identify molecular components that make up the smell of a common food: peanut butter odor (PB-O). These odor components, along with PB-O and a control food odor (banana, CTL-O), were delivered to human subjects during functional magnetic resonance imaging (fMRI), both before and after a lunch of peanut butter on crackers, as a way to induce olfactory sensory-specific satiety (Gottfried et al., 2003; Kringelbach et al., 2003; O'Doherty et al., 2000) (Figure 1). In this manner, we could track changes in satiety-related reward value both for an intact natural odor mixture and for its components, and relate these changes to fMRI activity in brain regions associated with odor and reward value processing. This design enabled us to make specific inferences about the neural underpinnings that support either elemental or configural coding schemes.

Three specific hypotheses were considered. First, if the value of a complex food odor is processed configurally, then satiety-related behavioral and neural effects should be unique to the mixture. Therefore mixture-specific changes in brain activity might be expected to occur in olfactory regions previously associated with configural coding, such as the posterior piriform cortex (PPC). Second, and conversely, if food odor value is coded elementally, then a subset of components should evoke satiety-related changes similar to the mixture, implying that the value representation embodied by the mixture is a function of some combination of its parts. One region that could maintain the fidelity of elemental olfactory information is the amygdala, which has access to representations of odorant identity through its direct inputs from discrete OB glomeruli (Buonviso et al., 1991; Haberly and Price, 1977; Miyamichi et al., 2011; Sosulski et al., 2011). As a third, hybrid hypothesis, configural and elemental processing might take place simultaneously in distinct circuits, implying that the olfactory system is capable of extracting behaviorally salient information from specific odorant components while also encoding the unified representation of the whole odor. A plausible neural substrate for mediating such a dual-processing stream is the OFC, which receives projections from both PC and amygdala (Carmichael et al., 1994; Carmichael and Price, 1995), and has been implicated in olfactory stimulus and satiety-related reward value coding (Gottfried and Zald, 2005; Schoenbaum and Eichenbaum, 1995; Small et al., 2008; Small et al., 2001).

RESULTS

Satiety-related effects: the whole odor

Using GC/MS technology equipped with a solid-phase microextraction (SPME) fiber for odor headspace analysis (Figure 1A), we identified 14 components from samples of

commercially available peanut butter odor (Figure 1B and see **Experimental Procedures**). Each of these components has been previously detected in experiments analyzing the volatile headspace of peanut samples (Chetschik et al., 2010; Liu et al., 2011; Ng et al., 2008). However, because these and other studies have identified significantly more than these 14 components in their mixture samples, we do not assume that our component set represents the complete molecular makeup of PB-O. Rather, we consider our set to constitute an experimentally tractable sample of the population of PB-O components with which to test hypotheses of configural and elemental mixture coding. Characterizing each component by its principal functional group, this set included 6 pyrazines, 5 aldehydes, and 3 “others”. High purity versions of these component odors, along with PB-O and CTL-O, were intermittently delivered to human participants while they underwent fMRI both before and after eating peanut butter to self-reported satiety (Figure 1C). Using an identical GC/MS analysis we found that the CTL-O odor consisted of only 3 molecular components (isoamyl acetate, amyl acetate, and ethyl butyrate), and thus did not share any components with the PB-O mixture.

Immediately before and after the feeding phase of the experiment, subjects provided ratings of “hunger”, “desire to eat”, “fullness”, and “satiety” on visual analog scales. These ratings confirmed that subjects were hungry when they arrived at the experiment and full when they finished eating (all p’s < 0.001, paired t-tests; Figure S1). After sniffing the odor on each trial, subjects provided ratings of either odor pleasantness or intensity, with ratings randomly presented such that the rating type could not be anticipated at the time of odor delivery. The behavioral efficacy of olfactory sensory-specific satiety was assessed by comparing the change in pleasantness rating from pre- to post-satiety for PB-O to that of CTL-O. This analysis revealed that the pleasantness of PB-O was significantly reduced after the feeding phase, compared to the CTL-O ($F_{1,10} = 4.26$, $p = 0.033$, one-tailed, interaction between odor condition and scanning session; repeated measures ANOVA) (Figure 2A). Using the same analysis we found that the satiety manipulation had no significant effect on perceived odor intensity ($F_{1,10} = 1.38$, $p = 0.47$; Figure S1), and did not influence sniff behavior (p’s > 0.32 for sniff volume, peak amplitude, and sniff duration; Figure S2). We thus established a behavioral sensory-specific satiety effect, whereby the appetitive reward value of the sated odor was significantly diminished compared to the non-sated food odor, similar to previous findings (Gottfried et al., 2003; O'Doherty et al., 2000; Rolls and Rolls, 1997).

We analyzed fMRI activity in seven regions of interest (ROIs) commonly associated with odor and reward value processing: anterior piriform cortex (APC), posterior piriform cortex (PPC), orbitofrontal cortex (OFC), amygdala (AM), anterior insula (AI), ventromedial prefrontal cortex (VMPFC), and ventral striatum (VS) (Figure 2B). ROIs were defined using a combination of anatomical and unbiased functional criteria (see **Experimental Procedures**). We first asked whether the behavioral satiety effect described above was mirrored by mean fMRI activity changes in any of these seven tested ROIs.

Utilizing an fMRI univariate analysis, we found a significant sensory-specific decrease in both OFC ($F_{1,10} = 11.33$, $p = 0.0072$; Figure 2C–D) and AI ($F_{1,10} = 4.89$, $p = 0.049$; Figure 2E–F). Satiety-related changes in mean fMRI activity were not observed in any other tested region (p’s > 0.73; Figure S3). Although there was no sensory-specific change in mean

activity in AM, we did observe a significant main effect of testing session in this region, such that the fMRI signal evoked by PB-O and CTL-O was significantly reduced after satiety ($F_{1,10} = 4.99$, $p = 0.050$; Figure S3). These findings are in accordance with previous studies demonstrating fMRI signatures of sensory-specific satiety in OFC and AI (Critchley and Rolls, 1996; Gottfried et al., 2003; Kringelbach et al., 2003; O'Doherty et al., 2000; Small et al., 2001; Sun et al., 2014). Moreover, the amygdala has been shown to process both negative and positively valenced stimuli, and is implicated in general processing of stimulus reward value (Baxter and Murray, 2002; Fontanini et al., 2009; Kadohisa and Wilson, 2006).

Given that OFC has direct anatomical connections with all other tested ROIs (Barbas and Pandya, 1989; Carmichael et al., 1994; Carmichael and Price, 1996), we next tested whether devaluation of the sated odor was associated with a change in functional coupling between OFC and these brain areas. To this end, we conducted a psychophysiological interaction (PPI) analysis to quantify BOLD signal coherence between an OFC seed region and each voxel in APC, PPC, AM, AI, VMPFC, and VS in both the pre- and post-satiety sessions (see **Experimental Procedures**). The OFC voxels used collectively as the seed region were the same as those reported in the univariate analysis above. We found a significant satiety-related modulation of connectivity between OFC and AM, such that the connectivity strength associated with PB-O was significantly decreased after satiety compared to CTL-O ($F_{1,10} = 4.61$, $p = 0.029$, one-tailed; Figure 2G). There were no satiety-related connectivity changes between OFC and any other tested region (p's > 0.47; Figure S3). Moreover, the spatial extent of this connectivity effect, calculated as the percentage of voxels within an ROI displaying a significant sensory-specific modulation of connectivity with OFC (at a liberal threshold of $p < 0.05$ uncorrected), was greater in AM than in any other tested region ($F_{2.03,20.31} = 6.05$, $p = 0.0085$; post-hoc t-tests, p's < 0.01 in pairwise comparisons between OFC and each of the other ROIs; Figure 2H–I). Although the threshold of $p < 0.05$ was chosen arbitrarily for this analysis, this effect was persistent (i.e., more significant voxels in AM than in the other tested regions) across a range of p-values between 0.01 and 0.1. Thus the satiety-related devaluation of PB-O was accompanied by a mean signal decrease in OFC as well as a modulation of functional connectivity between OFC and AM.

Notably, we did not observe satiety-related changes in mean activity in PPC using univariate analyses ($p = 0.46$). However, recent studies from our lab have employed multivariate techniques to show that distributed patterns of activity across PPC voxels encode both odor objects and their associated reward value (Howard et al., 2009; Li et al., 2008). We therefore conducted a multivoxel pattern analysis to test whether the satiety manipulation induced a sensory-specific modulation of fMRI ensemble activity in any of our tested regions. Linear correlations were calculated between pre-satiety and post-satiety patterns evoked by PB-O and compared to correlations between patterns evoked by CTL-O. In order to preserve the native spatial fidelity of the fMRI signal, correlations were calculated using patterns that were not spatially smoothed (see **Experimental Procedures**).

This analysis revealed a significant de-correlation, or divergence, between pre- and post-satiety PPC patterns evoked by PB-O compared to CTL-O ($t_{10} = 3.09$, $p = 0.012$, paired t-test on Fisher Z-transformed correlation coefficients; Figure 3A), but not in any other tested

region (p's > 0.20, Figure S3). Moreover, the magnitude of sensory-specific pattern shift in PPC was directly related to the behavioral sensory-specific satiety effect on a subject-by-subject basis ($r = -0.68$, $p = 0.021$, Pearson correlation) (Figure 3B,C). These findings demonstrate that stimulus-specific changes in the reward value of a natural food odor are directly related to a divergence in odorevoked pattern ensemble activity in PPC, a key olfactory region that is critical for object-level processing of olfactory stimuli (Gottfried, 2010; Wilson and Sullivan, 2011).

Satiety-related effects: odor components

The above results indicate that when a pleasurable food is eaten to satiety, the whole odor corresponding to that food is perceived as less pleasant, and elicits reduced mean fMRI activity in OFC and AI. Specific satiation to the full PB-O stimulus was also accompanied by functional decoupling of fMRI activity between OFC and AM, and by decorrelation of fMRI ensemble patterns in PPC. We next asked whether these effects were confined to the whole PB-O (consistent with configural coding), or could also be identified in discrete odorant components of the full odor mixture (consistent with elemental coding).

None of the 14 components was associated with a significant decrease in pleasantness rating from pre- to post-satiety, when compared to CTL-O (Figure 4A–B). However, when each component was tested against CTL-O in a session-by-odor interaction, four of the components evoked a significant sensory-specific decrease in mean OFC activity: 3-methyl butanal ("c3"; $F_{1,10} = 5.41$, $p = 0.042$), 2,5-dimethyl pyrazine ("c8"; $F_{1,10} = 11.61$, $p = 0.0067$), 2,3-dimethyl pyrazine ("c9"; $F_{1,10} = 6.52$, $p = 0.028$), and 3-ethyl-2,5-dimethyl pyrazine ("c13"; $F_{1,10} = 7.83$, $p = 0.019$; Figure 4C). A follow-up test comparing average pleasantness rating change across these 4 components (c3, c8, c9, c13) to the remaining 10 components revealed a significant difference ($t_{10} = 2.86$, p = 0.0085), suggesting that while no single component was sufficient to evoke a behavioral effect similar to the PB-O mixture, these four components in concert evoked significant satiety-related reward devaluation. Contrary to the element-based findings in OFC, when we examined component coding in AI, no PB-O component was associated with a significant satiety-related change in mean fMRI activity, either in the comparison to CTL-O (as was done with PB-O; repeated-measures ANOVA, p's > 0.13) or in the comparison of pre- to post-satiety (paired t-tests, p's > 0.23).

In order to determine whether satiety-related changes in OFC activity were related to initial differences among the components in OFC signal strength or perceptual ratings, we tested these measures using one-way ANOVAs in data from the pre-satiety session only. There was no significant difference across PB-O components in pre-satiety OFC signal ($F_{13,130} = 1.25$, $p = 0.29$). While the components differed in pre-satiety pleasantness ($F_{13,130} = 3.87$, $p < 0.001$) and intensity ($F_{13,130} = 4.96$, $p < 0.001$), there was no difference when we averaged these pre-satiety ratings across the presumably salient components (c3, c8, c9, c13) and tested them against ratings averaged across the non-salient components (pre-satiety pleasantness: $t_{10} = 0.87$, $p = 0.41$; pre-satiety intensity: $t_{10} = 0.157$, $p = 0.88$). These results suggest that the component specific changes in OFC signal were not driven merely by

disparity among the components in initial OFC signal or subjective pleasantness or intensity ratings.

As reported above, there was a decrease in mean AM activity for both PB-O and CTL-O (see Figure S3), but no sensory-specific effect in this region. Therefore, we did not test component responses against CTL-O in this region as was done in the OFC. Instead we simply tested whether the mean post-satiety fMRI signal was significantly different from the pre-satiety signal for each component. Using this analysis, we found that two of the components evoked a significant decrease in AM activity from pre- to post-satiety: 2–5 dimethyl pyrazine ("c8"; $t_{10} = 1.85$, $p = 0.047$), and 3-ethyl-2,5-dimethyl pyrazine ("c13"; $t_{10} = 2.10$, $p = 0.031$; Figure 4D).

Given that PB-O was associated with a sensory-specific decoupling of functional activity between OFC and AM after satiety, we also tested whether this effect could be observed for any of the PB-O components. For this analysis we averaged component-specific connectivity parameters across voxels that exhibited a significant sensory-specific change in connectivity for PB-O vs. CTL-O ($p < 0.05$). One subject had no significant voxels from this analysis, so the following results were averaged across 10 subjects. We found a significant sensory-specific decrease in connectivity between the OFC seed region and AM for 3-methyl butanal ("c3"; $F_{1,9} = 5.43$, $p = 0.045$) and 3-ethyl-2,5-dimethyl pyrazine ("c13"; $F_{1,9} = 4.02$, $p = 0.038$, one-tailed; Figure 4E).

These results demonstrate that a subset of components evoked neural effects similar to the whole odor in which they are found, providing evidence that the satiety-related reward value of a natural odor mixture is coded elementally by a subset of its parts. Given that satiety-related changes in perceived pleasantness of PB-O closely mirrored changes in mean OFC activity (see Figure 2C), we also considered whether there might be a systematic relationship between pleasantness and OFC activity across the full set of components. To this end, we regressed satiety-related changes in mean OFC activity, mean AM activity, and OFC/AM functional connectivity against pleasantness rating change across the full set of 14 components. In each case we found a significant positive correlation between neural effects and behavioral ratings (mean OFC signal change: $r = 0.72$, $p = 0.004$; mean AM signal change: $r = 0.63$, $p = 0.016$; OFC/AM connectivity change: $r = 0.78$, $p = 0.0011$; Figure 5A–C). By comparison, there was no significant correlation between any of these effects and component-specific changes in perceived intensity (p's > 0.1, Figure S4). These findings suggest that while a subset of components behaves like the mixture itself, the remaining components may also contribute to reward value coding in a graded way, such that the mixture effect is a combination of effects across all mixture components.

Whereas a subset of PB-O components elicited similar mean activity effects to the whole odor in OFC and AM, no component evoked a significant shift in ensemble patterns of voxel activity in PPC (p's > 0.32, paired t-tests), when compared to the whole odor mixture response (Figure S5). Moreover, there was no relationship between satiety-related PPC pattern change and pleasantness rating across the component set ($r = -0.28$, $p = 0.34$; Figure S5). Thus the sensoryspecific pattern changes were specific to the whole PB-O, suggesting that the effects observed in PPC constitute a more configural processing mode.

Physical and perceptual characteristics of odor mixture components

The demonstration that sensory-specific satiety has a direct impact on the components comprising the sated food odor led us to consider whether specific physical features could explain the contribution of a given odor component to the observed behavioral and fMRI effects. To this end, we used commercially available software to tabulate 32 molecular descriptors for each PB-O component (see **Experimental Procedures**). By conducting principal components analysis and *k*-means clustering on these descriptors, we determined that the components fell into three groups: 1) the 5 aldehydes plus "c2" and "c14"; 2) the 6 pyrazines; and 3) "c5" (Figure 6A). When averaging effects across components in Groups 1 and 2, we found no significant differences between these groups in terms of satiety-related changes in perceived pleasantness, mean OFC activity, mean AM activity, or functional connectivity between OFC and AM (p's > 0.22; Figure S6). Thus the molecular features of a given odor mixture component are not apparently related to their propensity to exhibit satiety-related value signaling similar to the mixture itself.

We also explored whether olfactory perceptual features could inform the relationship between the odor components and the satiety-related effects. In order to index odor quality, ratings of perceptual similarity between each PB-O component and the PB-O mixture were collected in a separate testing session prior to scanning. Across the set of components, similarity to the PB-O mixture (i.e., how "peanut butter-like" each component was) was significantly correlated with satiety-related changes in component pleasantness ($r = -0.74$, $p = 0.0023$; Figure 6B). There was also a trend towards significance in the correlation between component similarity to PB-O and satiety-related changes in mean OFC activity ($r = -0.49$, $p = 0.083$, data not shown). However, there was no relationship between component similarity to PB-O and concomitant satiety-related changes in mean AM activity ($r = -0.40$, $p = 0.16$), OFC-AM connectivity ($r = -0.39$, $p = 0.19$), or PPC pattern shifts ($r = 0.13$, $p = 0.65$). These results suggest that there was some relationship between component similarity to PB-O and its propensity to evoke mixture-like changes in pleasantness rating and mean OFC fMRI signal.

DISCUSSION

A key function of the brain is to extract behaviorally relevant information from complex realworld stimuli. Sensory systems can adopt different processing strategies to contend with this complexity. In configural processing, stimulus parts are integrated into perceptual wholes that convey meaning; for example, the sight of a stalking lion, or the smell of its hide. In elemental processing, the stimulus parts themselves may hold salience; for example, specific visual details of the lion's face, or specific odor components contained in the lion's scent. Data presented here indicate that the human olfactory system engages both configural and elemental strategies to encode odor salience, with dissociable brain areas supporting each of these processing modes.

Our study utilized an olfactory paradigm of sensory-specific satiety, in which the pleasantness of an odor is reduced when its corresponding food has been eaten to satiety. In this way we were able to determine whether satiety-induced changes in odor pleasantness (reward value) could be isolated at the level of individual components, and, if so, which

brain regions were involved. Critically, a GC/MS system enabled us to identify 14 odor components of a complex natural food aroma, peanut butter (PB-O), which is widely enjoyed in humans and holds behavioral relevance for this species. Similar GC/MS approaches have been used in animal models to test brain activity to components of natural odors holding behavioral salience for rodent and insect species (Lin et al., 2005; Riffell et al., 2009).

Direct evidence for elemental representations of a natural food odor was found in the analysis of PB-O components: a small subset of the 14 components was associated with satiety-related response decreases in both the OFC and AM. Moreover, a functional connectivity analysis revealed a satiety-specific reduction of odor-evoked coupling between OFC and AM for two components (3-ethyl-2,5-dimethyl pyrazine and 3-methyl butanal). Finally, across the full set of components, satiety-related changes in pleasantness correlated with corresponding fMRI changes in OFC activity, AM activity, and OFC-AM connectivity. These effects were not influenced by mere component differences in pre-satiety pleasantness or intensity, nor did they appear to be related to particular physicochemical characteristics – indeed, while three of the components mediating fMRI changes were pyrazine molecules, another three pyrazines had no influence on value-related representations in either OFC or AM.

Although speculative, the unique behavioral and neural response profile exhibited by these putatively relevant components may be due to their more consistent representation in naturally occurring variants of peanut odor mixtures. In this hypothetical scenario, repeated experience with such variants could possibly “tune” the system towards more efficiently extracting relevant value information from the most stable mixture components. In a follow-up GC/MS analysis, we found that 12 of the 14 PB-O components identified in our original peanut butter samples were present in four additional commercially available natural peanut butter brands (see **Experimental Procedures**). Interestingly, the two components that were not consistently found in these other brands (c2, 2-butanone, and c12, trimethyl pyrazines) were not included in the subset of “salient” PB-O components. However, this analysis did not provide conclusive evidence for or against the hypothesis that behaviorally relevant components in particular are represented more consistently across varieties of peanut butter odors, and a more comprehensive study of odor mixture variants with known genetic origins would be necessary to fully address this question.

Insofar as certain components in an odor mixture may preferentially embody the behavioral salience of the mixture itself, it is imperative that component-specific signal fidelity be preserved in projections from the olfactory bulb to downstream cortical areas. Anatomical tracing studies have shown that projections from distinct glomeruli in the OB terminate in spatially invariant subregions of the amygdala (Miyamichi et al., 2011; Sosulski et al., 2011). As both an integral site for processing odor hedonic value (Gottfried et al., 2002; Royet et al., 2003; Zald and Pardo, 1997) and a downstream target of appetite-suppressing neurons from the brainstem (Carter et al., 2013), the amygdala thus constitutes a biologically plausible substrate in which component-specific value signals related to satiety state could be represented. The demonstration of elemental odor processing in human amygdala is compatible with these anatomical findings and provides novel functional support for the role

of this brain area in having access to component-level value information about a complex natural odor mixture. That we observed a satiety-related decrease in mean signal intensity for both PB-O and CTL-O suggests that value-related coding in this region is not sensory-specific, but may act as a more permissive gateway through which interconnected brain regions could access hedonic information about a mixture or a subset of its components.

Conversely, evidence for olfactory configural processing was identified in PPC. Distributed ensemble patterns of odor-evoked PPC activity diverged from pre- to post-satiety for the whole PB-O, compared to CTL-O, but such pattern changes were not observed for any of the PB-O components. That a qualitative reorganization of odor coding in PPC was restricted to the whole mixture accords well with rodent and human data, which increasingly indicate that this region supports configural object-level representations of odor qualities and categories (Barnes et al., 2008; Howard et al., 2009; Kadohisa and Wilson, 2006; Li et al., 2008). Interestingly, the fact that sensory-specific satiety modulated the PPC pattern representation in response to the *same* PB-O stimulus implies that a change in the reward value of an olfactory object has a fundamental effect on how that object is encoded and perceived.

The findings in PPC can also be understood in context of its known anatomical and physiological properties. In contrast to the point correspondence between the OB and AM, piriform cortex receives diffuse and distributed inputs from individual mitral cells in the bulb, without apparent topographical organization (Chapuis and Wilson, 2012; Ghosh et al., 2011; Miyamichi et al., 2011; Rennaker et al., 2007; Sosulski et al., 2011; Stettler and Axel, 2009). The divergent nature of these projections would make it difficult to map odor-evoked activity patterns in the PPC onto component-specific representations in the bulb. In effect, the elemental composition of an odor mixture becomes inaccessible at the level of PPC. That said, satiety-related changes associated with PB-O could theoretically generalize to odor components sharing perceptual similarity with the whole stimulus mixture (Guttman and Kalish, 1956; Kahnt et al., 2012). In this manner, the reward value of a particularly peanut-buttery component might evoke pattern effects similar to PB-O itself.

We did not observe any relationship between pattern effects in PPC and component similarity to PB-O (see Fig S5), perhaps owing to the fact that even the most peanut-like component (c13, 3- ethyl 2,5-dimethyl pyrazine) was rated only modestly similar to PB-O (+2.5, on a scale from −10 to +10). We did, however, find that component similarity to PB-O was directly related to satiety-related component pleasantness rating changes (see Fig. 6B), and trended toward a significant relationship with mean OFC signal change. In addition, the most similar component, c13, was associated with satiety effects in OFC, AM, and the functional connectivity between the two (see Fig. 4C–E). That odor components with greater perceptual similarity to peanut butter are more likely to evoke effects comparable to the mixture implies that some degree of generalization occurred. The range of stimulus generalization could be intrinsically limited to those components embedded within the odor mixture itself. As a form of within-mixture generalization, perceptual similarity to the whole odor would determine which components are targets of sensory-specific satiety, enhancing the complexity of signal inputs available for downstream processing. Alternatively, stimulus generalization could be extrinsic to the set of mixture components,

such that sensory-specific olfactory devaluation would transfer to any odor sharing perceptual attributes, irrespective of whether that odor was part of the original mixture. This process by which sensory-specific odor devaluation broadly generalizes to perceptually related odors would help diversify selection of nutritionally unique foodstuffs. Distinguishing between these two scenarios is difficult in the present experiment, though in future studies, and in line with experimental paradigms in rodent models (Barnes et al., 2008; Chapuis and Wilson, 2012), it would be intriguing to systematically remove specific components from the whole PB-O as a method of assessing intrinsic vs. extrinsic generalization effects.

Evidence for configural coding of olfactory reward value was also found in AI. In contrast to the profile observed in OFC, satiety-related changes in mean AI fMRI activity were restricted to the whole PB-O mixture, and were not observed for any PB-O components. Previous studies of insula function suggest that the anterior portion in particular is involved in processing the behavioral salience of sensory stimuli and coordinating with other large scale brain networks to orient attentional resources towards those stimuli (Corbetta and Shulman, 2002; Seeley et al., 2007; Touroutoglou et al., 2012). Insofar as the behavioral salience of the sated odor was diminished after satiety, the findings in AI would be consistent with the idea that attention is shifted towards non-sated food odors that retain behavioral salience. Further evidence for such a role for AI comes from a rodent study in which rats with AI lesions continued to press a lever to receive a devalued food after satiety, suggesting that this region is critical for updating associations between food-related stimuli and their associated rewards (Balleine and Dickinson, 2000).

Here we have shown that the human olfactory system can process the olfactory reward value of a natural food odor by simultaneously employing elemental processes in AM and configural processes in PPC. Previous studies in non-human model systems have found evidence for both processing modes in the olfactory system (Livermore et al., 1997; Meyer and Galizia, 2012), providing empirical support for the proposed theory that odor-driven behavior arises from a combination of two primary mechanisms (Wilson and Stevenson, 2006). In the “physicochemical” mode, simple odors or individual molecules within an odor mixture are sufficient to drive stereotypical or innate behavioral responses. In the “memory-based” mode, odor mixtures are synthesized into unitary, perceptual wholes that are associated with objectlevel perception and are susceptible to experience-based plasticity. Taken together, the results presented here provide the first evidence that such dual mode processing is in place in the human brain.

The demonstration of both elemental and synthetic forms of odor processing highlights the perceptual “multiplexing” capacity of the human olfactory system to extract different forms of information from odor stimuli (Gire et al., 2013). Interestingly, our data suggest that OFC may reside at the core of these processes: from pre- to post-satiety, the whole PB-O stimulus and several of the PB-O components were associated with a decrease in mean OFC activity and with a functional decoupling between OFC and AM. This scheme is in accordance with olfactory learning studies in rodents demonstrating that disrupting functional connectivity between OFC and AM can impair the ability to update stimulus-reward associations (Baxter et al., 2000; Saddoris et al., 2005; Schoenbaum et al., 2003). Based on its central role in

olfactory processing (Gottfried and Zald, 2005; O'Doherty et al., 2000; Schoenbaum and Eichenbaum, 1995) and its bidirectional connectivity with both AM and PPC (Carmichael et al., 1994; Carmichael and Price, 1995), the OFC is well positioned to integrate both configural and elemental streams of information. Access to component-specific olfactory representations in the amygdala could provide a mechanism for OFC to rapidly and efficiently "read out" value-related information from small subsets of odor mixture molecules, whereas access to object-level representations in PPC would offer a way to link value signals in OFC with the specific quality, or identity, of the odor. Importantly, both processing modes would contain information about the reward value of the mixture, and either mode could be engaged during a given task to optimize reward-related behavior.

The idea that a unique subset of PB-O components may signal the reward value of the whole mixture has intriguing implications. Taking this concept to an extreme, one might predict that spiking the four identified components into *any odor mixture* should confer added value (literally) to that mixture. Even the presence of these four components in other food smells might alter behavioral acceptance of these foods, despite the fact that they share little perceptual similarity with PB-O. Such scenarios could be counterproductive, with the undesirable side effect of enhancing consumption of foodstuffs that may not be optimal. Rather, an arrangement where elemental and configural systems cooperate to form integrated representations of value and quality, with perturbations in one system inducing changes in the other, would offer a more stable framework for guiding food-based behaviors. As a higher-order olfactory region with access to both elemental and configural information, the OFC may act as a coincidence detector, such that for a behavioral response to be driven by a given stimulus, it must evoke recognizable representations at both the object and component level, conferring the ability to respond to stimuli not just with overlapping physical or perceptual features, but with a combination of both.

EXPERIMENTAL PROCEDURES

Identification of peanut butter odor components

PB-O components were identified from the gaseous headspace of a sample of commercially available peanut butter (Smucker's® Organic Creamy, Orrville, OH) using gas chromatography/mass spectrometry (GC/MS) equipment (7890A GC system, 5975C MSD, Agilent Technologies, Santa Clara, CA). For each sample analysis, 2g of peanut butter prepared in a 20mL vial was transferred by a robotic autosampler (Gerstel, Inc., Linthicum, MD) to a 60°C agitation chamber. A solid-phase microextraction (SPME, Supelco, Sigma-Aldrich Corp, St. Louis, MO) fiber was then injected through a septum in the vial, exposed to the sample headspace for 30 minutes, and then transferred to the injection port of an HP-5ms (5% phenyl 95% methylpolysiloxane) GC column where it was held at 270°C for one minute to allow for desorption of the volatiles into the column. The GC oven temperature was held at 35°C for 1 minute, increased to 60°C at 5°C/min., held at 60°C for 5 minutes, and increased to 230°C at 15°C/min. Three different types of SPME fibers were used (CAR/PDMS, DVB/CAR/PDMS, PDMS/DVB), each of which has a coating designed for optimal adsorption of a distinct range of molecular features. For each fiber type, three identical GC/MS runs described above were conducted, each using a fresh sample of peanut

butter. Chromatogram peaks were identified offline using the NIST mass spectral library in ChemStation software. A component was considered to be reliably identified if it was present on all three repetitions of one of the 3 SPME fibers. The same analysis technique was used to identify molecular components of the control odor (Old Hickory Brand banana extract, Punxsutawney, PA), and the four other tested brands of peanut butter odor (Skippy Natural, Hormel Foods, Austin, MN; Simply Jif, Smucker Company, Orrville, OH; Krema Natural, Krema Group, Dublin, OH; and Roundy's Natural, Roundy's Supermarkets, Milwaukee, WI).

Participants

Thirteen right-handed, non-smoking participants with no history of neurological disorders gave informed consent to take part in this experiment according to protocols approved by the Northwestern University Institutional Review Board. Due to technical difficulties encountered during scanning, 2 participants were excluded from the study.

Stimuli and delivery

High purity synthetic versions of the 14 identified PB-O components were obtained from Sigma- Aldrich and prepared for testing at low concentrations (1–5%, dissolved in mineral oil or propylene glycol). PB-O was prepared from a sample of peanut butter oil, and CTL-O was prepared from a sample of banana extract. For pre-scanning behavioral testing, odorants were prepared in amber bottles. During scanning, odorants were delivered using a custom built olfactometer that diverts air at a flow rate of 2.5L/min. through vessels containing polyethylene pellets soaked in liquid odorants (Gottfried et al., 2002).

Pre-scanning behavioral ratings

Participants were cued by a computer screen to sniff one of the 14 PB-O components prepared in an amber bottle and rate how similar it was to PB-O on a visual analog scale (anchors "not at all alike" and "identical"). Each component was rated twice, and subjects were allowed to sniff a sample of PB-O *ad libitum* as they gave their ratings.

fMRI scanning parameters

Gradient-echo T2-weighted echoplanar images were acquired with a Siemens Trio 3T scanner using parallel imaging and a 12-channel head-coil (repetition time, 2s; echo time, 20ms; matrix size, 128 × 120 voxels; field-of-view, 220 × 206mm; in-plane resolution, 1.72 × 1.72mm; slice thickness, 2mm; gap, 1mm; acquisition angle, 30° rostral to the intercommissural line). A 1-mm^3 isotropic T1-weighted MRI scan was also acquired.

fMRI scanning experiment

Subjects were instructed to skip the meal prior to arriving at the experiment and thus arrive in a hungry state. In the pre-satiety phase of the experiment subjects underwent four 10-minute fMRI runs during which each of the 16 odors was presented three times in pseudorandom order. On each trial subjects were cued to make a sniff and then rate either the pleasantness or intensity of the odors. On a third of the trials there was no rating. The three rating types were pseudorandomly paired with the odors such that they could not be

anticipated at the time of odor presentation. Ratings of odor pleasantness (anchors "extremely pleasant" and "extremely unpleasant") and odor intensity (anchors "extremely weak" and "extremely strong") were made on a visual analog scale using an MR-compatible trackball mouse. The post-satiety phase was identical to the pre-satiety phase except that the stimulus order was independently randomized. In the feeding phase, subjects were given a newly opened jar of peanut butter and a plate of lowsodium crackers, and allowed to eat until self-reported satiety.

Respiratory monitoring

Subjects were loosely affixed with respiratory effort bands to monitor breathing (Gottfried et al., 2002). Sniff waveforms were extracted for each trial, sorted by condition, and normalized within scanning session. Sniff volume, peak amplitude, and duration were calculated separately for each trial and then averaged across trials for group statistical analysis (Figure S2).

Region of interest (ROI) definition

APC, PPC, and AM were manually drawn according to a neuroanatomical atlas (Mai et al., 2004) on each subject's T1 anatomical scan using MRIcron (mricro.com). The OFC ROI was defined as a subregion of the entire OFC, centered near the intersection of the medial, lateral, and transverse orbital sulci according to a meta-analysis of odor-evoked activity in human OFC (Gottfried and Zald, 2005). For AI, VMPFC, and VS, regional centroids (coordinates) were defined in standardized MNI (Montreal Neurological Institute) space, according to a metaanalysis of human fMRI studies reporting brain activation related to subjective value judgments (Bartra et al., 2013). These coordinates were: AI (−30, 22, −6; and 32, 20, −6); VMPFC (2, 46, −8); and VS (−12, 12, −6; and 12, 10, −6). MNI coordinates were converted to each subject's native T1 space, and a sphere with a radius of 4 voxels was grown around each converted coordinate to define the ROI. The T1 scan was co-registered to the mean realigned functional image using SPM8 (www.fil.ion.ucl.ac.uk/spm/) on a subject-by-subject basis, and the resulting spatial transformation parameters were applied to the ROIs.

fMRI data analysis

All functional scans across both pre- and post-satiety phases were spatially realigned to the first scan of the first imaging run using SPM8 to correct for head movement. fMRI activity for each scan and voxel in the ROIs was extracted from the functional volumes using custom scripts written in Matlab (Natick, MA). To remove the effects of sensory habituation, for each voxel the time series of fMRI activity in a scanning run was temporally detrended by subtracting the 2^{nd} order trend from the data. Data were then sorted by ROI and odor condition, and averaged across the first 8 TRs (12.08s) after stimulus onset for each trial. Noisy voxels were removed from the dataset by testing an ANOVA across all 16 conditions in each ROI using the pre-satiety data only. Because all subsequent analyses considered interactions between condition and scanning session, this voxel selection technique remained independent and did not bias further results. Voxels with a p-value > 0.5 were discarded and the remaining data were analyzed in two ways. We first tested for satiety-

related effects carried in the mean signal averaged across voxels in an ROI. Second, we tested whether the satiety manipulation caused changes in multivoxel patterns of odor-evoked BOLD activity in a given region. In both cases, we first tested for an effect specific to PB-O vs. CTL-O, and then tested if any of the PB-O components evoked a similar effect.

Mean signal analysis

For the mean analysis, within each subject, ROI, scanning session, and condition, the fMRI signal was averaged across trials and voxels that survived the liberally thresholded omnibus ANOVA described above. For the PB-O vs. CTL-O analysis (see Figure 2B) we tested for satiety-related differences in a 2-way repeated measures ANOVA with subjects as repetitions and condition and scanning session (pre- and post-satiety) as factors. For the PB-O component analysis (see Figure 4C), each component was tested separately in a similar 2-way ANOVA against CTL-O.

Multi-voxel pattern analysis

Data were averaged across trials (but not voxels), resulting in a single pattern of voxel activity for each subject, ROI, condition, and scanning session. Each pattern was z-scored across voxels such that no subsequent effects from this analysis could be explained by mere differences in mean activity levels across conditions. Linear correlations were then calculated between pre- and post-satiety patterns for each condition. Group effects were calculated using paired *t*-tests on the Fisher *z*-transformed correlation coefficients ($z = 0.5*\ln[(1+r)/(1-r)]$).

Functional connectivity analysis

We used the generalized form of the psycho-physiological interaction (PPI) model (Friston et al., 1997; McLaren et al., 2012) to test for satiety-related changes in functional connectivity between an OFC seed region and all voxels in the remaining ROIs. The seed region was defined as the set of OFC voxels that passed the omnibus ANOVA used to select voxels for the mean signal analysis. We then constructed a general linear model (GLM) for each subject consisting of 32 “psychological regressors” (one for each of the 16 odor conditions and 2 scanning sessions), 2 “physiological regressors” (the average OFC activity in each of the 2 sessions), and 6 regressors for the head movement parameters derived from the motion correction process. Odor onsets were modeled as events and convolved with the canonical hemodynamic response function. The PPI parameters estimated from this model thus reflected the correlation between the average OFC activity and every scanned voxel in the brain. Parameters corresponding to voxels in the remaining ROIs were sorted by condition and scanning session, averaged across voxels within the ROI, and tested at the group level for satiety-related interaction effects.

Molecular feature analysis

The 32 molecular descriptors used in this analysis (tabulated using Dragon software, Talete, Milan, Italy) were identified in a previous study as maximally accounting for odor-evoked neural activity changes across model species, neural recording methods, and odorants

(Haddad et al., 2008). Principal components analysis, *k*-means clustering, and silhouette value (Rousseeuw, 1987) calculation were performed using Matlab scripts.

Statistics

Based on previous studies of satiety and reward value processing, we had strong directional hypotheses regarding expected changes in the behavioral and univariate fMRI effects (Critchley and Rolls, 1996; Gottfried et al., 2003; O'Doherty et al., 2000; Rolls and Rolls, 1997), as well as OFC-AM connectivity (Baxter et al., 2000; Saddoris et al., 2005; Schoenbaum et al., 2003) Statistical significance was assessed using repeated-measures ANOVA (for session-by-condition interactions) and paired *t*-tests (for comparisons between two conditions) with a threshold of $p < 0.05$, two-tailed, unless otherwise noted. Component effects (see Figure 4C–E) were corrected for multiple comparisons using false discovery rate correction with a *q*-value set to 0.1 ($p < 0.029$, one-tailed, 14 comparisons).

Supplementary Material

Refer to Web version on PubMed Central for supplementary material.

Acknowledgments

This work was supported with NIH funding to J.D.H. (5F31DC013500) and to J.A.G. (R01DC010014), supplemental NIH funding to J.A.G. through the American Recovery and Reinvestment Act (ARRA) of 2009 (3R01DC010014-01S1), and a Seed Grant from the Brain Research Foundation to J.A.G. (BRF SG2010-07 and SG2011-06). We would like to thank Thorsten Kahnt for providing helpful comments to the manuscript, and Katherine Khatibi for assistance in acquiring the fMRI data.

REFERENCES

Balleine BW, Dickinson A. The effect of lesions of the insular cortex on instrumental conditioning: evidence for a role in incentive memory. J. Neurosci. 2000; 20:8954–8964. [PubMed: 11102506]

Barbas H, Pandya DN. Architecture and intrinsic connections of the prefrontal cortex in the rhesus monkey. J. Comp. Neurol. 1989; 286:353–375. [PubMed: 2768563]

Barnes DC, Hofacer RD, Zaman AR, Rennaker RL, Wilson DA. Olfactory perceptual stability and discrimination. Nat. Neurosci. 2008; 11:1378–1380. [PubMed: 18978781]

Bartra O, McGuire JT, Kable JW. The valuation system: a coordinate-based meta-analysis of BOLD fMRI experiments examining neural correlates of subjective value. Neuroimage. 2013; 76:412–427. [PubMed: 23507394]

Baxter MG, Murray EA. The amygdala and reward. Nat. Rev. Neurosci. 2002; 3:563–573. [PubMed: 12094212]

Baxter MG, Parker A, Lindner CC, Izquierdo AD, Murray EA. Control of response selection by reinforcer value requires interaction of amygdala and orbital prefrontal cortex. J. Neurosci. 2000; 20:4311–4319. [PubMed: 10818166]

Buonviso N, Revial MF, Jourdan F. The Projections of Mitral Cells from Small Local Regions of the Olfactory Bulb: An Anterograde Tracing Study Using PHA-L (Phaseolus vulgaris Leucoagglutinin). Eur. J. Neurosci. 1991; 3:493–500. [PubMed: 12106481]

Carmichael ST, Clugnet MC, Price JL. Central olfactory connections in the macaque monkey. J. Comp. Neurol. 1994; 346:403–434. [PubMed: 7527806]

Carmichael ST, Price JL. Limbic connections of the orbital and medial prefrontal cortex in macaque monkeys. J. Comp. Neurol. 1995; 363:615–641. [PubMed: 8847421]

Carmichael ST, Price JL. Connectional networks within the orbital and medial prefrontal cortex of macaque monkeys. J. Comp. Neurol. 1996; 371:179–207. [PubMed: 8835726]

Carter ME, Soden ME, Zweifel LS, Palmiter RD. Genetic identification of a neural circuit that suppresses appetite. Nature. 2013; 503:111–114. [PubMed: 24121436]

Chapuis J, Wilson DA. Bidirectional plasticity of cortical pattern recognition and behavioral sensory acuity. Nat. Neurosci. 2012; 15:155–161. [PubMed: 22101640]

Chetschik I, Granvogl M, Schieberle P. Quantitation of key peanut aroma compounds in raw peanuts and pan-roasted peanut meal. Aroma reconstitution and comparison with commercial peanut products. J. Agric. Food Chem. 2010; 58:11018–11026. [PubMed: 20866052]

Corbetta M, Shulman GL. Control of goal-directed and stimulus-driven attention in the brain. Nat. Rev. Neurosci. 2002; 3:201–215. [PubMed: 11994752]

Critchley HD, Rolls ET. Hunger and satiety modify the responses of olfactory and visual neurons in the primate orbitofrontal cortex. J. Neurophysiol. 1996; 75:1673–1686. [PubMed: 8727405]

Fontanini A, Grossman SE, Figueroa JA, Katz DB. Distinct subtypes of basolateral amygdala taste neurons reflect palatability and reward. J. Neurosci. 2009; 29:2486–2495. [PubMed: 19244523]

Friston KJ, Buechel C, Fink GR, Morris J, Rolls E, Dolan RJ. Psychophysiological and modulatory interactions in neuroimaging. Neuroimage. 1997; 6:218–229. [PubMed: 9344826]

Ghosh S, Larson SD, Hefzi H, Marnoy Z, Cutforth T, Dokka K, Baldwin KK. Sensory maps in the olfactory cortex defined by long-range viral tracing of single neurons. Nature. 2011; 472:217–220. [PubMed: 21451523]

Gire DH, Whitesell JD, Doucette W, Restrepo D. Information for decision-making and stimulus identification is multiplexed in sensory cortex. Nat. Neurosci. 2013; 16:991–993. [PubMed: 23792942]

Gottfried JA. Central mechanisms of odour object perception. Nat. Rev. Neurosci. 2010; 11:628–641. [PubMed: 20700142]

Gottfried JA, Deichmann R, Winston JS, Dolan RJ. Functional heterogeneity in human olfactory cortex: an event-related functional magnetic resonance imaging study. J. Neurosci. 2002; 22:10819–10828. [PubMed: 12486175]

Gottfried JA, O'Doherty J, Dolan RJ. Encoding predictive reward value in human amygdala and orbitofrontal cortex. Science. 2003; 301:1104–1107. [PubMed: 12934011]

Gottfried JA, Zald DH. On the scent of human olfactory orbitofrontal cortex: meta-analysis and comparison to non-human primates. Brain Res. Brain Res. Rev. 2005; 50:287–304. [PubMed: 16213593]

Guttman N, Kalish HI. Discriminability and stimulus generalization. J. Exp. Psychol. 1956; 51:79–88. [PubMed: 13286444]

Haberly LB, Price JL. The axonal projection patterns of the mitral and tufted cells of the olfactory bulb in the rat. Brain Res. 1977; 129:152–157. [PubMed: 68803]

Haddad R, Khan R, Takahashi YK, Mori K, Harel D, Sobel N. A metric for odorant comparison. Nat. Methods. 2008; 5:425–429. [PubMed: 18376403]

Honey RC, Iordanova MD, Good M. Associative structures in animal learning: dissociating elemental and configural processes. Neurobiol. Learn. Mem. 2014; 108:96–103. [PubMed: 23769767]

Howard JD, Plailly J, Grueschow M, Haynes JD, Gottfried JA. Odor quality coding and categorization in human posterior piriform cortex. Nat. Neurosci. 2009; 12:932–938. [PubMed: 19483688]

Kadohisa M, Wilson DA. Separate encoding of identity and similarity of complex familiar odors in piriform cortex. Proc. Natl. Acad. Sci. U. S. A. 2006; 103:15206–15211. [PubMed: 17005727]

Kahnt T, Park SQ, Burke CJ, Tobler PN. How glitter relates to gold: similarity-dependent reward prediction errors in the human striatum. J. Neurosci. 2012; 32:16521–16529. [PubMed: 23152634]

Kanwisher N, McDermott J, Chun MM. The fusiform face area: a module in human extrastriate cortex specialized for face perception. J. Neurosci. 1997; 17:4302–4311. [PubMed: 9151747]

Kay LM, Crk T, Thorngate J. A redefinition of odor mixture quality. Behav. Neurosci. 2005; 119:726–733. [PubMed: 15998193]

Kringelbach ML, O'Doherty J, Rolls ET, Andrews C. Activation of the human orbitofrontal cortex to a liquid food stimulus is correlated with subjective pleasantness. Cereb. Cortex. 2003; 13:1064–1071. [PubMed: 12967923]

Laing DG, Francis GW. The capacity of humans to identify odors in mixtures. Physiol. Behav. 1989; 46:809–814. [PubMed: 2628992]

Li W, Howard JD, Parrish TB, Gottfried JA. Aversive learning enhances perceptual and cortical discrimination of indiscriminable odor cues. Science. 2008; 319:1842–1845. [PubMed: 18369149]

Lin DY, Zhang SZ, Block E, Katz LC. Encoding social signals in the mouse main olfactory bulb. Nature. 2005; 434:470–477. [PubMed: 15724148]

Liu X, Jin Q, Liu Y, Huang J, Wang X, Mao W, Wang S. Changes in volatile compounds of peanut oil during the roasting process for production of aromatic roasted peanut oil. J. Food Sci. 2011; 76:C404–C412. [PubMed: 21535807]

Livermore A, Hutson M, Ngo V, Hadjisimos R, Derby CD. Elemental and configural learning and the perception of odorant mixtures by the spiny lobster Panulirus argus. Physiol. Behav. 1997; 62:169–174. [PubMed: 9226358]

Mai, JK.; Assheuer, J.; Paxinos, G. Atlas of the Human Brain. 2nd edn. San Diego: Elsevier Academic Press; 2004.

McLaren DG, Ries ML, Xu G, Johnson SC. A generalized form of context-dependent psychophysiological interactions (gPPI): a comparison to standard approaches. Neuroimage. 2012; 61:1277–1286. [PubMed: 22484411]

Melchers KG, Shanks DR, Lachnit H. Stimulus coding in human associative learning: flexible representations of parts and wholes. Behav. Processes. 2008; 77:413–427. discussion 451-413. [PubMed: 18031954]

Meyer A, Galizia CG. Elemental and configural olfactory coding by antennal lobe neurons of the honeybee (Apis mellifera). J. Comp. Physiol. A Neuroethol. Sens. Neural. Behav. Physiol. 2012; 198:159–171. [PubMed: 22083110]

Miyamichi K, Amat F, Moussavi F, Wang C, Wickersham I, Wall NR, Taniguchi H, Tasic B, Huang ZJ, He Z, et al. Cortical representations of olfactory input by trans-synaptic tracing. Nature. 2011; 472:191–196. [PubMed: 21179085]

Ng EC, Dunford NT, Chenault K. Chemical characteristics and volatile profile of genetically modified peanut cultivars. J. Biosci. Bioeng. 2008; 106:350–356. [PubMed: 19000610]

O'Doherty J, Rolls ET, Francis S, Bowtell R, McGlone F, Kobal G, Renner B, Ahne G. Sensory-specific satiety-related olfactory activation of the human orbitofrontal cortex. Neuroreport. 2000; 11:893–897. [PubMed: 10757540]

Pearce JM. Similarity and discrimination: a selective review and a connectionist model. Psychol. Rev. 1994; 101:587–607. [PubMed: 7984708]

Rennaker RL, Chen CF, Ruyle AM, Sloan AM, Wilson DA. Spatial and temporal distribution of odorant-evoked activity in the piriform cortex. J. Neurosci. 2007; 27:1534–1542. [PubMed: 17301162]

Rescorla, RA.; Wagner, AD. A theory of Pavlovian conditioning: variations in the effectiveness of reinforcement and nonreinforcement. In: Black, AH.; Prokasy, WF., editors. In Classical Conditioning II: Current Theory and Research. New York: Appleton-Century-Crofts; 1972. p. 64-99.

Riffell JA, Lei H, Hildebrand JG. Neural correlates of behavior in the moth Manduca sexta in response to complex odors. Proc. Natl. Acad. Sci. U. S. A. 2009; 106:19219–19226. [PubMed: 19907000]

Rolls ET, Rolls JH. Olfactory sensory-specific satiety in humans. Physiol. Behav. 1997; 61:461–473. [PubMed: 9089767]

Rousseeuw PJ. Silhouettes: A graphical aid to the interpretation and validation of cluster analysis. J. Comput. Appl. Math. 1987; 20:53–65.

Royet JP, Plailly J, Delon-Martin C, Kareken DA, Segebarth C. fMRI of emotional responses to odors: influence of hedonic valence and judgment, handedness, and gender. Neuroimage. 2003; 20:713–728. [PubMed: 14568446]

Saddoris MP, Gallagher M, Schoenbaum G. Rapid associative encoding in basolateral amygdala depends on connections with orbitofrontal cortex. Neuron. 2005; 46:321–331. [PubMed: 15848809]

Saper CB, Chou TC, Elmquist JK. The need to feed: homeostatic and hedonic control of eating. Neuron. 2002; 36:199–211. [PubMed: 12383777]

Schoenbaum G, Eichenbaum H. Information coding in the rodent prefrontal cortex. I. Single-neuron activity in orbitofrontal cortex compared with that in pyriform cortex. J. Neurophysiol. 1995; 74:733–750. [PubMed: 7472378]

Schoenbaum G, Setlow B, Saddoris MP, Gallagher M. Encoding predicted outcome and acquired value in orbitofrontal cortex during cue sampling depends upon input from basolateral amygdala. Neuron. 2003; 39:855–867. [PubMed: 12948451]

Seeley WW, Menon V, Schatzberg AF, Keller J, Glover GH, Kenna H, Reiss AL, Greicius MD. Dissociable intrinsic connectivity networks for salience processing and executive control. J. Neurosci. 2007; 27:2349–2356. [PubMed: 17329432]

Shepherd GM. Smell images and the flavour system in the human brain. Nature. 2006; 444:316–321. [PubMed: 17108956]

Small DM, Veldhuizen MG, Felsted J, Mak YE, McGlone F. Separable substrates for anticipatory and consummatory food chemosensation. Neuron. 2008; 57:786–797. [PubMed: 18341997]

Small DM, Zatorre RJ, Dagher A, Evans AC, Jones-Gotman M. Changes in brain activity related to eating chocolate: from pleasure to aversion. Brain. 2001; 124:1720–1733. [PubMed: 11522575]

Snitz K, Yablonka A, Weiss T, Frumin I, Khan RM, Sobel N. Predicting odor perceptual similarity from odor structure. PLoS Comput. Biol. 2013; 9:e1003184. [PubMed: 24068899]

Sosulski DL, Bloom ML, Cutforth T, Axel R, Datta SR. Distinct representations of olfactory information in different cortical centres. Nature. 2011; 472:213–216. [PubMed: 21451525]

Stettler DD, Axel R. Representations of odor in the piriform cortex. Neuron. 2009; 63:854–864. [PubMed: 19778513]

Sun X, Veldhuizen MG, Wray AE, de Araujo IE, Sherwin RS, Sinha R, Small DM. The neural signature of satiation is associated with ghrelin response and triglyceride metabolism. Physiol. Behav. 2014

Touroutoglou A, Hollenbeck M, Dickerson BC, Feldman Barrett L. Dissociable large-scale networks anchored in the right anterior insula subserve affective experience and attention. Neuroimage. 2012; 60:1947–1958. [PubMed: 22361166]

Whalen PJ, Kagan J, Cook RG, Davis FC, Kim H, Polis S, McLaren DG, Somerville LH, McLean AA, Maxwell JS, Johnstone T. Human amygdala responsivity to masked fearful eye whites. Science. 2004; 306:2061. [PubMed: 15604401]

Wilson, DA.; Stevenson, RJ. Learning to smell: olfactory perception from neurobiology to behavior. Baltimore, MD: The Johns Hopkins University Press; 2006.

Wilson DA, Sullivan RM. Cortical processing of odor objects. Neuron. 2011; 72:506–519. [PubMed: 22099455]

Yoshida I, Mori K. Odorant category profile selectivity of olfactory cortex neurons. J. Neurosci. 2007; 27:9105–9114. [PubMed: 17715347]

Zald DH, Pardo JV. Emotion, olfaction, and the human amygdala: amygdala activation during aversive olfactory stimulation. Proc. Natl. Acad. Sci. U. S. A. 1997; 94:4119–4124. [PubMed: 9108115]

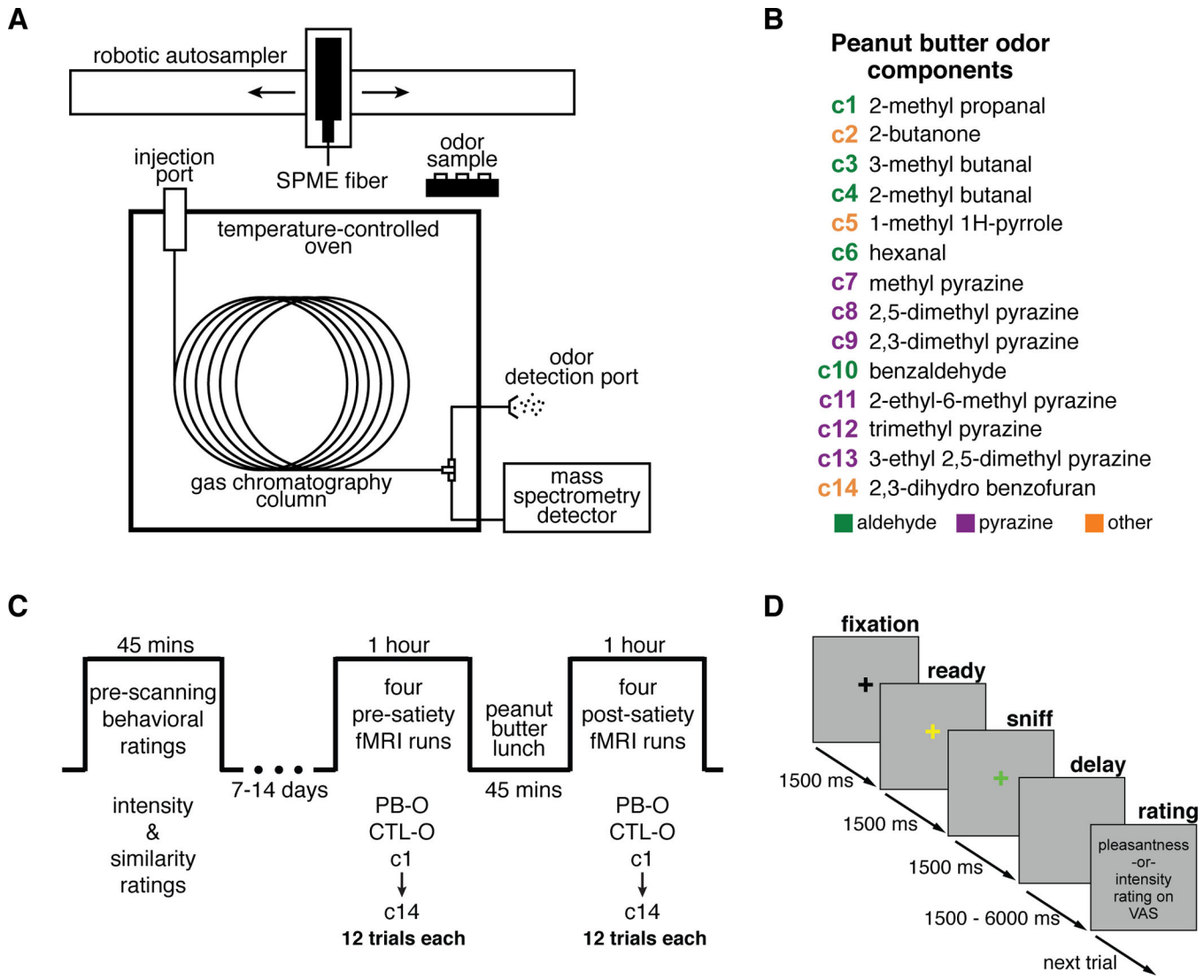

Figure 1. Peanut butter odor components and experimental design

(**A**) Schematic of GC/MS equipment. The SPME fiber was exposed to the headspace of a peanut butter sample for 30 minutes before injection into GC column. (**B**) PB-O components identified by GC/MS analysis, listed in the order they came off the GC column, color coded by principal functional group. (**C**) Experimental timeline. In the pre-scanning phase, subjects rated the intensity of each of the 16 odor stimuli twice. These ratings were used to adjust odor concentrations in an attempt to minimize perceived intensity differences during the scanning session. Subjects also provided ratings of perceptual similarity between PB-O and each of its components in this phase. (**D**) Trial sequence. After a 1500ms “ready” cue, subjects were cued to sniff by presentation of a green crosshair during the 1500ms odor delivery. Then, after a variable delay, a rating prompt was shown.

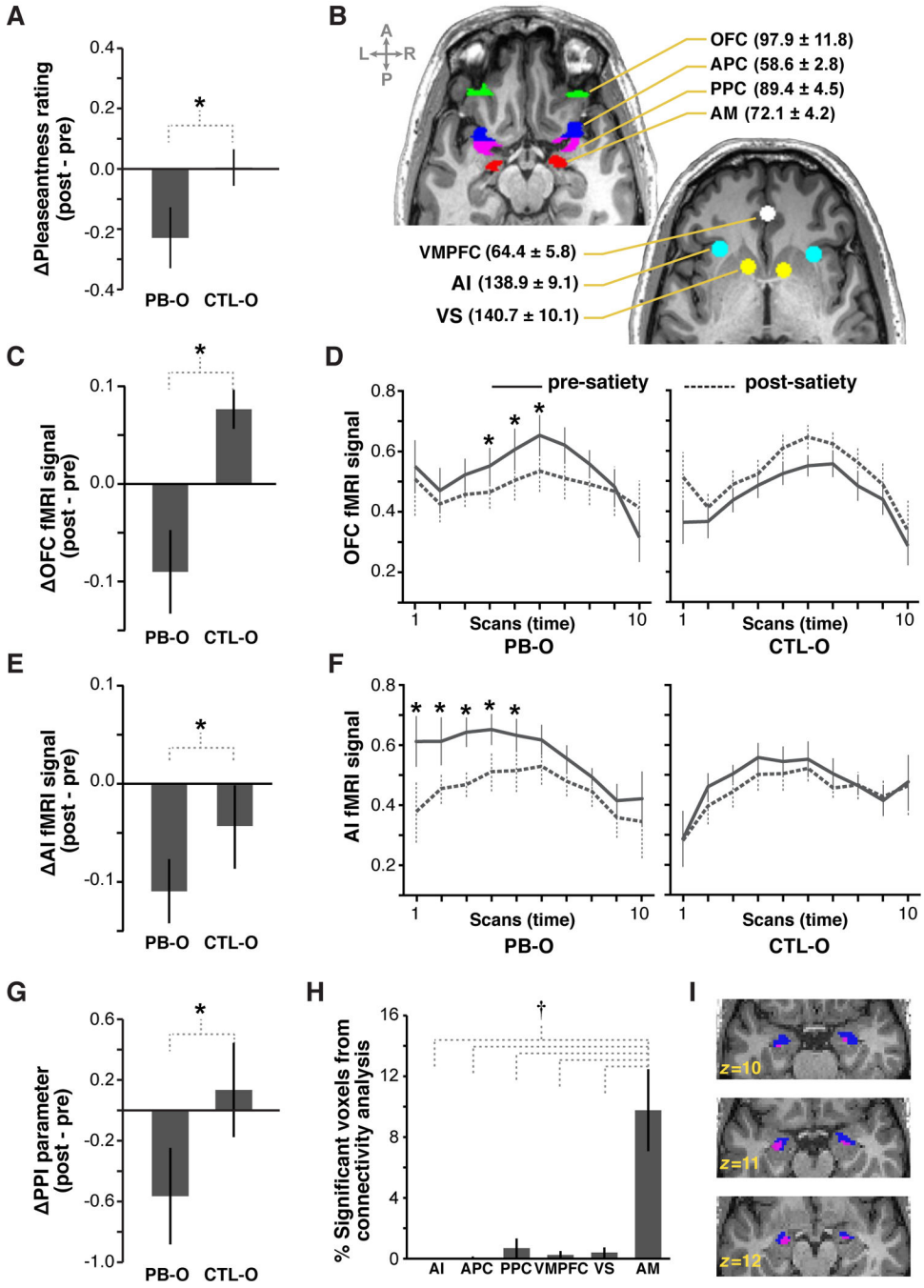

Figure 2. Sensory-specific satiety effects in relation to the whole odor

(**A**) Change in pleasantness rating for PB-O and CTL-O from pre- to post-satiety. (**B**) Regions of interest from a representative subject overlaid on axial slices of a T1-weighted anatomical scan. Average numbers of voxels that passed the unbiased omnibus ANOVA (± s.e.m.) are in parentheses. (**C**) Satiety-related change in mean OFC activity. (**D**) Time course of OFC activity, starting from onset of odor delivery. One scan = 1.51s. (**E,F**) Satiety-related change in mean and fMRI time course of AI activity. (**G**) Change in functional connectivity strength between OFC and AM from pre- to post-satiety. (**H**) Percentage of voxels in tested

ROIs showing significant sensoryspecific modulation of functional connectivity with OFC. (**I**) Cluster of voxels (pink) from three consecutive axial slices of a representative subject showing significant sensory-specific modulation of functional connectivity between OFC and AM ($p < 0.05$, repeated measures ANOVA), overlaid on the anatomical AM ROI (blue). All error bars represent across-subject standard error of the mean (s.e.m.). *$p < 0.05$, repeated measures ANOVA; $^{\dagger}p < 0.05$, post-hoc *t*-tests.

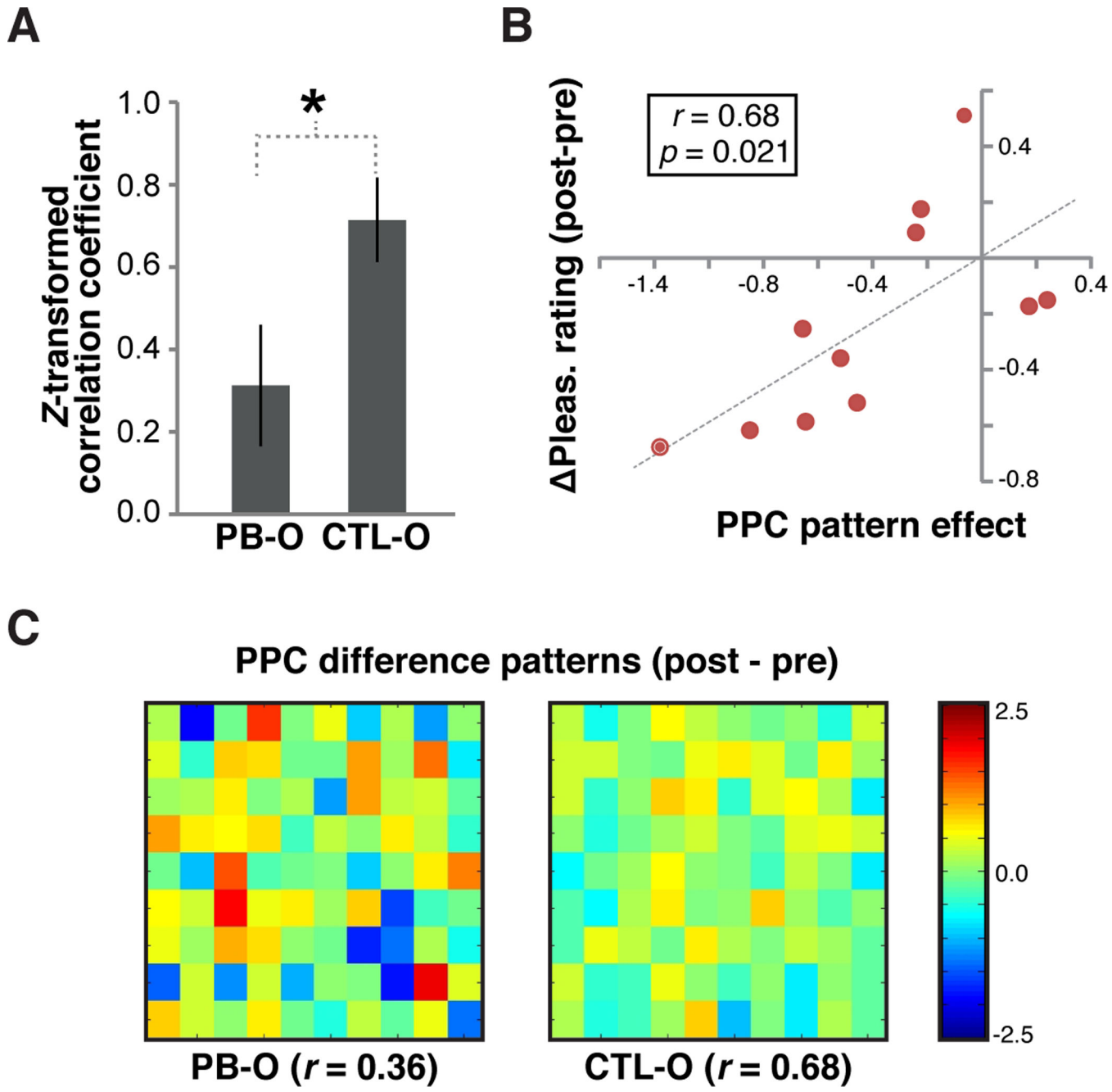

Figure 3. Satiety-related effects on fMRI pattern ensemble activity evoked by the whole odor

(**A**) Subject-average correlation (Fisher *z*-transformed) between pre-satiety patterns and post-satiety patterns for PB-O and CTL-O in PPC, indicating greater pattern divergence for PB-O. (**B**) Relationship between PPC pattern effect (PB-O correlation coefficient minus CTL-O correlation coefficient) and satiety-related behavioral effects. Each dot on the scatter plot represents data from one subject. (**C**) Difference maps from a representative subject. Each pixel on the map represents one voxel in the PPC ROI. Pre-satiety PPC patterns of activity were subtracted from post-satiety patterns. The correlation value between the two

patterns is shown below the difference map. Error bars = across-subject s.e.m., *$p < 0.05$, paired *T*-test.

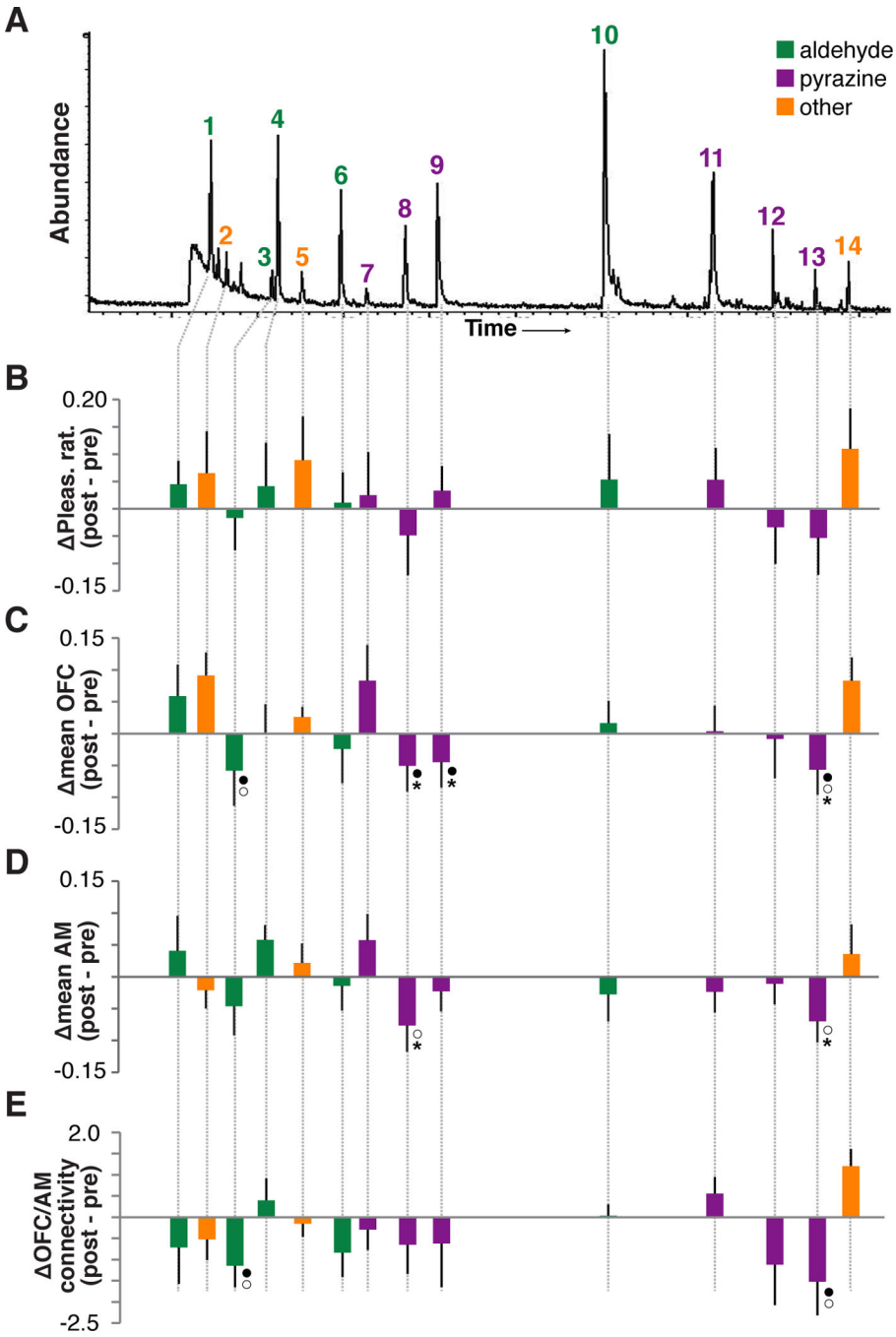

Figure 4. Satiety-related effects in response to the odorant components

(**A**) Chromatograph obtained from one GC/MS analysis of a peanut butter odor sample. Each labeled peak indicates an identified PB-O component. Note that "abundance" on the *y*-axis does not reflect the relative concentration of each identified component in the mixture. See Fig.1B for chemical identities of the 14 components. (**B–E**) Satiety-induced changes in pleasantness (**B**), mean OFC activity (**C**), mean AM activity (**D**), and functional connectivity between OFC and AM (**E**) for each PB-O component. Error bares = across-subject s.e.m; ●*p*

< 0.05, repeated measures ANOVA, condition-by-session interaction; ○$p < 0.05$ paired *t*-test, pre- vs. post-satiety; *corrected for false discovery rate (FDR) with $q = 0.1$.

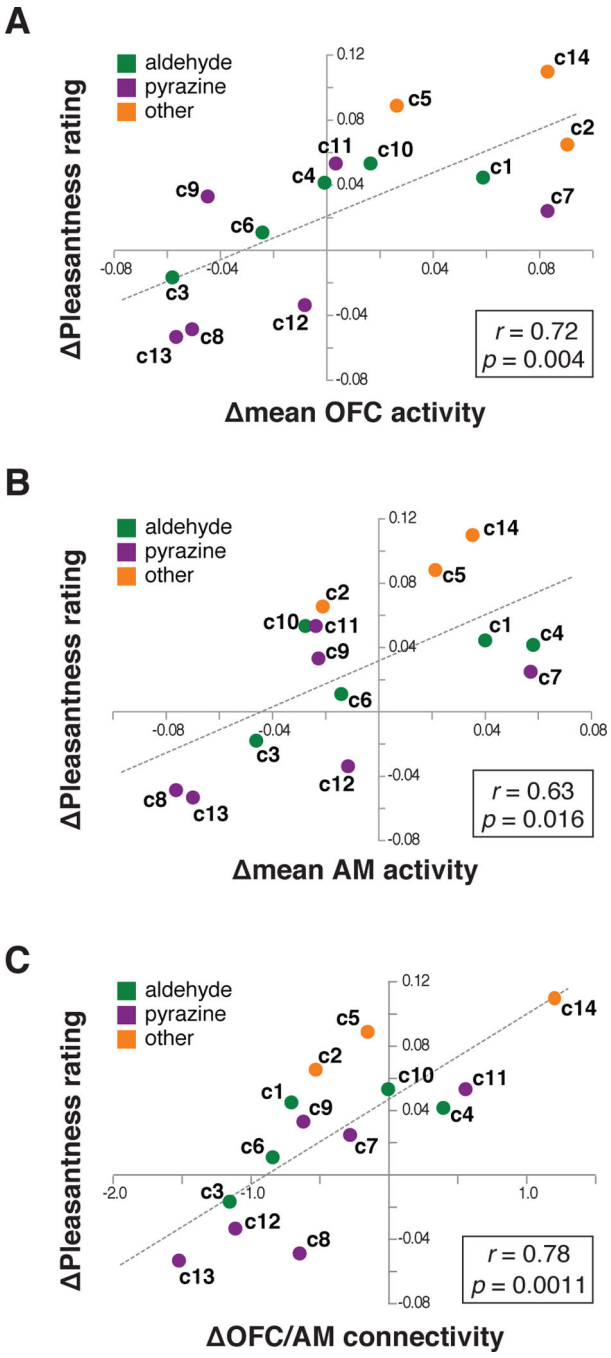

Figure 5. Relationship between neural effects and pleasantness change in PB-O components

Across the set of PB-O components, satiety-related change in pleasantness was significantly correlated with change in mean OFC activity (**A**), mean AM activity (**B**), and change in functional connectivity between OFC and AM (**C**).

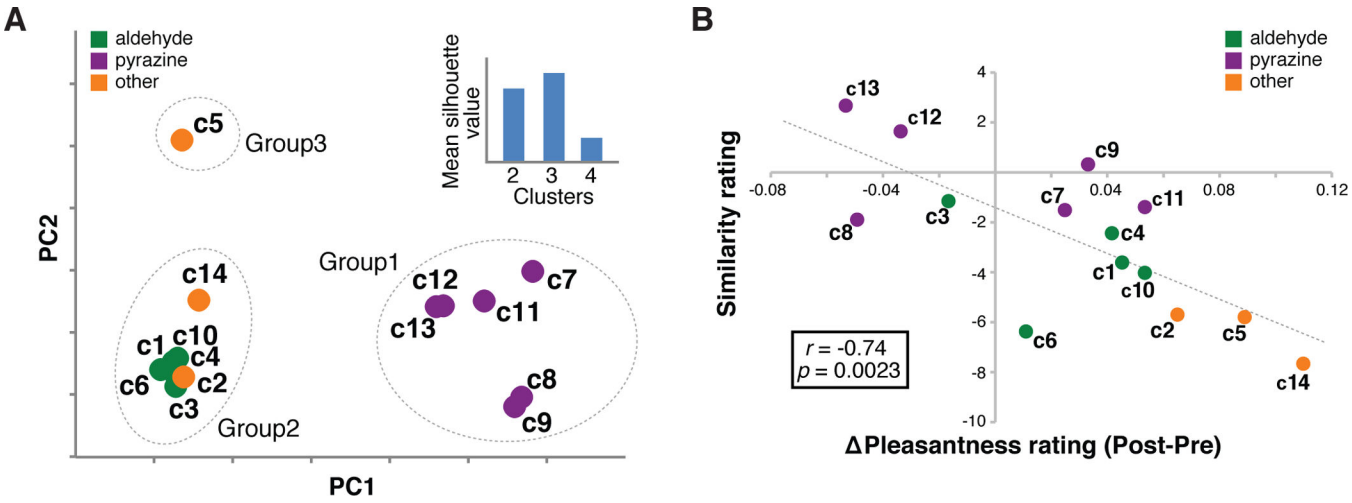

Figure 6. Physicochemical and perceptual aspects of PB-O components

(**A**) The first two principal components (PCs) are plotted for each PB-O component. Dotted circles around components reflect the best clustering solution arrived at using *k*-means clustering. The mean silhouette value in the inset reflects how far apart the points in each cluster are to those in other clusters. A larger value indicates better cluster separation, justifying the use of three clusters in subsequent analyses. (**B**) Correlation between component-specific change in pleasantness rating and the pre-satiety rating of perceptual similarity between components and PB-O.